Nonlocal effect of plasma resonances on the electron energy-distribution function in microwave plasma columns

O. Boudreault, S. Mattei, L. Stafford, J. Margot, M. Moisan, R. Khare, and V. M. Donnelly

Phys. Rev. E **86**, 015402 — Published 19 July 2012

DOI: 10.1103/PhysRevE.86.015402

Non-local effect of plasma resonances on the electron energy distribution function in microwave plasma columns

O. Boudreault, S. Mattei, L. Stafford*, J. Margot, and M. Moisan

Département de Physique, Université de Montréal, Montréal, Québec, Canada H3C 3J7

R. Khare and V. M. Donnelly

Departement of Chemical and Biomolecular Engineering, University of Houston, Houston, Texas, USA 77204

ABSTRACT

Spatially-resolved trace-rare-gas-optical-emission-spectroscopy was used to analyze the electron energy distribution function (EEDF) in low-pressure, argon plasma columns sustained by surface waves. At frequencies >1 GHz, in the microwave-sustained region, the EEDF departs from a Maxwellian, characterized by a depletion of low-energy electrons and a high-energy tail, whereas in the field-free zone, the EEDF is Maxwellian. Abnormal behavior of the EEDF results from the acceleration of low-energy electrons due the conversion of surface waves into volume plasmons at the resonance point where the plasma frequency equals the wave frequency and their absorption by either collisional or Landau damping.

* Corresponding author : luc.stafford@umontreal.ca

Recent advances in large-area plasma sources sustained by microwave electromagnetic (EM) fields, intended for various technological applications (e.g., etching and deposition of thin films), have raised many questions on the physics driving electron heating and wave-particle interactions in such discharges. In general, electrons in high-frequency plasmas are accelerated by the electric field and energy is redistributed to the plasma particles through electron-neutral collisions. In the near-collisionless regime where the frequency for electron-neutral collisions, ν, is much lower than the field angular frequency, ω, electron heating can also result from momentum transfer from high-voltage moving sheaths [1,2,3]. This stochastic electron heating is particularly important in plasmas created and maintained by a radio frequency electric field not exhibiting a wave nature such as capacitively-coupled plasmas. On the other hand, when the electric field supporting the plasma is an EM wave (e.g., a surface wave) that carries the power away from the wave launching region [4,5], the self-consistent interaction between the wave and the plasma results in an overdense discharge (i.e. electron angular plasma frequency ω_{pe} higher than ω) that can give rise to a number of interesting phenomena, including modulation instability and possibilities of soliton formation [6], wave breaking [7], and electron cyclotron resonance [8]. A few studies further pointed out the development of electron plasma resonances near the discharge boundaries where $\omega \approx \omega_{pe}$, resulting from the spatial inhomogeneity of the plasma [9]. These resonances result in large and sharp peaks of the electric field component parallel to the density gradient [10,11,12]. On the basis of hydrodynamic and kinetic calculations, it was proposed that the enhancement of the electric field could result in enhanced Joule heating [10] as well as the generation of fast electrons [13].

The existence and precise role of plasma resonances nonetheless continues to be a subject of debate, due to a lack of convincing and comprehensive experimental validation [14]. Indirect

evidence by Langmuir probe measurements have been reported, such as the presence of local peaks in the plasma–floating potential near the end of a plasma column [15], and the detection of high-energy electrons near the fused-silica windows in both tubular and planar-type surface-wave discharges [16,17,18,19]. It is well-known, however, that probe measurements are problematic in wave-sustained plasmas since metallic electrodes perturbs the self-consistent wave-plasma behavior. In addition, the contribution of high-energy electrons to the total probe current is hindered by the large ion current.

In this Letter, a non-intrusive, trace-rare-gas-optical-emission-spectroscopy (TRG-OES) technique highly sensitive to the detection of high-energy electrons is used to analyze the electron energy distribution function (EEDF) along a low-pressure, argon plasma column sustained in the microwave regime by EM surface waves. In the large-area, planar-type configurations used in many industry-driven applications, the EM field is stationary and often exhibits a multimode behavior, making fundamental investigations of the physics driving the electron dynamics difficult due to the complexity of the field distribution. In contrast, in the long, tubular configuration used in this study, the wave is a traveling wave and monomode propagation is readily achievable [20]. From our spatially-resolved measurements of the EEDF performed over a wide range of frequencies, it is concluded that the non-local electron dynamics in the overdense region of surface-wave plasmas is strongly linked to the excitation of volume plasmons near the discharge boundary at the resonance point where $\omega_p=\omega$ and their absorption by either collisional or Landau damping.

Most of our experiments were carried out in a 6 mm i.d. fused silica discharge tube evacuated by a turbomolecular pump. As detailed below, selected experiments were also performed in a fused silica tube tapering up from 6 mm i.d. to 25 mm i.d. In both systems, the

EM surface wave was excited in the small portion of the tube, using a gap-type wave launcher. A surfatron device [21] was used for experiments in the 600 to 2450 MHz frequency range while a Ro-box unit [22] was utilized to sustain plasmas at lower frequencies. The product of the frequency f times the tube radius R was always $<<2$ GHz cm, therefore ensuring that only the azimuthally symmetric mode of wave propagation (i.e., the mode for which the EM wave field intensity does not vary azimuthally) could be excited [20]. An argon flow rate of 20 standard cubic centimeters per minute (sccm) was mixed with 1 sccm of rare gases contained in a premixed-gas bottle (40% Ne and 20% each for Ar, Kr and Xe) to allow TRG-OES measurements. Plasma emission was collected by an optical fiber equipped with a collimator directed perpendicularly to the discharge tube axis, and monitored using an intensity-calibrated optical spectrometer.

In TRG-OES, the electron temperature is determined by measuring the emission line intensities coming from the $2p_x$ levels (Paschen's notation) of rare gases (here Ne, Kr and Xe) inserted in trace amounts, and comparing them to values computed from a model using the known electron-impact cross sections and branching ratios [23]. By selecting appropriate emission lines, an electron "temperature" characterizing an assumed Maxwellian distribution in a specific electron energy range can be determined for different energy segments of the EEDF. Three groups of emission lines were considered in this study, leading to three temperatures designated as low, high and tail. The first one, T_e^{low}, was obtained using a set of five Kr and Xe lines that are mainly excited by electron impact from the $^3P_{0,2}$ metastable levels (see ref. 23). The difference in energy between these metastable states and the emitting $2p_x$ levels being only of a few eVs, T_e^{low} is thus representative of the low-energy portion of the EEDF. T_e^{high} was determined using a set of six lines from Kr and Xe for which the upper levels are populated mainly by electron-impact excitation directly from the ground states (see ref. 23), requiring

electron energies of > 9.6-12.3 eV, i.e. the high-energy part of the EEDF. Finally, the high-energy tail of the EEDF was represented by a "tail temperature", T_e^{tail}, determined using the same emission lines as for T_e^{high} but with the addition of the Ne $2p^{10}$– $1s^4$ transition at 585.2 nm (the energy of the Ne $2p^{10}$ level is 19 eV above ground state and the contribution from stepwise excitation from the metastable states is negligible). Since Ar was the main plasma gas, none of its very intense emission lines were used due to radiation trapping effects [24]. If the EEDF were truly Maxwellian, then the use of different sets of emission lines gives an identical electron temperature. On the other hand, if different electron temperatures are found, then it is possible to determine how the EEDF departs from a Maxwellian.

Figure 1 shows the electron temperatures for a 50 mTorr argon plasma column. For f=100 MHz, $T_e^{low} \approx T_e^{high} \approx T_e^{tail} \simeq 4$ eV, suggesting that the EEDF is a Maxwellian. On the other hand, as the EM field frequency increases, both T_e^{low} and T_e^{tail} increase while T_e^{high} remains constant. At microwave frequencies, the EEDF thus has a distinct, three-temperature form with a steeper slope for the energy segments concerning low-energy electrons ($T_e^{low} > T_e^{high}$) and very high-energy electrons ($T_e^{tail} > T_e^{high}$). Hence, even with the relatively high ionization degree (~1 %) achieved in microwave-sustained plasmas, electron-electron collisions appear insufficient to ensure a Maxwellian distribution [25].

The average electron temperature $<T_e>$ can be calculated using a zero-dimensional model assuming that charged particles are created by electron-impact ionization on the ground state and are lost by ambipolar diffusion to the reactor walls. With this reasonable assumption for plasmas operated in the mTorr pressure range, the electron temperature depends only on the discharge gas pressure and nature and on plasma dimensions, yielding[26]

$$T_e = \frac{E_{iz}}{\ln\left(n_g \Lambda A_{iz}/u_B\right)}, \qquad (1)$$

where E_{iz} and A_{iz} are parameters in the expression for the ionisation rate coefficient $k=A_{iz}\exp(-E_{iz}/T_e)$, n_g is the neutral gas number density, u_B is the Bohm velocity, and Λ is an effective plasma length for positive ion diffusion given by $(1/\Lambda)^2=(\pi/L)^2+(2.405/R)^2$ for a cylindrical tube of length L and radius R. For a 50 mTorr, Ar plasma with $L>>R$= 3 mm, T_e = 4 eV, consistent with the data in Fig. 1 at low operating frequencies. Even though the "temperature" of the electrons in the intermediate range of energy, T_e^{high}, remains more or less constant from 100 MHz to 2.45 GHz, one still expects from the increase of the other two characteristic temperatures (Fig. 1) higher average electron energies at high operating frequencies. From the measurements of T_e^{low}, T_e^{high}, and T_e^{tail}, it is, however, difficult to construct the full EEDF with enough precision to determine whether the mean electron energy satisfy Eq. (1) at all frequencies. Nonetheless, by doing so using the approach in ref. [27], we obtained a $<T_e>$ value of 5-6 eV at 2.45 GHz. The slightly higher mean electron energies can probably be explained by a depletion of the number density of Ar neutrals available for ionization, due to the much higher electron densities at 2.45 GHz than at 100 MHz. For example, for $<T_e>$=6 eV and a typical radially-integrated electron number density of 3×10^{12} cm^{-3} along the surface-wave, argon plasma column at 2.45 GHz, the electron pressure accounts for 25 % of the total pressure, reducing the neutral atom pressure to 35 mTorr (we assume a neutral gas temperature of 300 K [28]). Given the corresponding 25% reduction in n_g, Eq. (1) predicts $<T_e>$=5 eV, consistent with our approximate averaging over the 3 energy segments of 5-6 eV at 2.45 GHz.

The data presented in Fig. 1 further suggests that raising the wave frequency induces a depletion in the number of low-energy electrons with respect to a single maxwellian of T_e = 4 eV ($T_e^{low} > T_e^{high}$) as well as the generation of fast electrons ($T_e^{tail} > T_e^{high}$). Several mechanisms can induce abnormal electron heating and thus yield non-Maxwellian EEDF. Stochastic electron

heating due to oscillating plasma sheaths cannot be invoked in microwave discharges: for the sheath to oscillate, the characteristic time for the sheath formation (~$2\pi/\omega_{pe}$) must be much shorter than the wave period $T = 2\pi/\omega$. While this is the case in radiofrequency plasmas (ω/ω_{pe}~500 at 13.56 MHz), the time for sheath formation in microwave discharges is at most comparable to, but not much shorter than the wave period. Since the wave oscillations are too fast for the sheath to follow, there should be no significant stochastic heating related to sheath oscillations. In addition, in the microwave regime, the excursion lengths per oscillating cycle are generally much smaller than the plasma dimensions. On the other hand, giving the high number densities of electrons (~10^{12} cm^{-3}) and Ar atoms in metastable and resonant states (~10^{12} cm^{-3}) in 2.45 GHz plasmas, one might expect superelastic collisions to play an important role in the electron heating. This possibility was investigated through kinetic simulations using the Boltzmann code provided by Hagelaar and Pitchford [29]. As shown in Fig. 2, even multiplying the cross sections for superelastic collisions by a factor of 100 with respect to published values introduces only small changes on the EEDF.

As mentioned above, the presence of high-intensity electric fields near the discharge boundaries in spatially-inhomogeneous surface wave plasmas due to the development of electron plasma resonances at $\omega \approx \omega_{pe}$ was theoretically predicted to produce suprathermal electrons [13]. This could possibly be attributed to transit-time heating during the electron transit time τ across the resonance peak of width Δ [10,16]. Transit-time heating occurs mostly when $\omega\tau \approx 1$ (for $\omega\tau >> 1$, the electron oscillates in the field without gaining energy until a collision disrupts its oscillation while for $\omega\tau << 1$ the electron is travelling too fast to experience the resonant field) [30]. For $\omega = 2\pi \times 2.45$ GHz and an estimated resonance width $\Delta = 2\times10^{-4}$ cm [10] for 50 mTorr Ar plasma with a radially-integrated electron number density of 10^{12} cm^{-3}, this criterion

corresponds to an electron velocity $u = \omega \Delta = 3 \times 10^6$ cm s^{-1}, i.e. an electron energy of 2.5 meV. Consequently, only very low-energy electrons could eventually be accelerated to the tenth of eV, indicating that transit-time heating through the resonant layer cannot explain the depletion of low-energy electrons in the few eV range described by T_e^{low} and the generation of electrons in the tens of eV given by T_e^{tail}.

As theoretically proposed by Aliev *et al.*[31], fast electron generation could result from the resonant conversion of long-wavelength electromagnetic surface waves into short-wavelength electrostatic Langmuir waves (volume plasmons) and their absorption by either collisional or Landau damping. To play an important role, these waves would need wavelengths much smaller than the plasma diameter, i.e., ~0.1-0.6 mm for our conditions. For f=2.45 GHz, this corresponds to phase velocities in the 2-15 $\times 10^7$ cm s^{-1} range and thus to electron energies between 0.1 and 6 eV. These low-energy electrons could therefore be accelerated to form the high-energy tail seen in the experiments. On the other hand, for f=100 MHz, if a similar resonant conversion occurred, the corresponding phase velocities would be 1-6 $\times 10^6$ cm s^{-1}, i.e. much lower electron energies. Similarly to transit-time heating, this would play only a minor role on the electron dynamics, which again is consistent with our experimental observations. In addition, at 100 MHz, the plasma tends to become more collisional (ν/ω increases) such that the resonance is less pronounced and thus the resonant wave conversion less likely [32].

Figure 3 presents the radial profile of T_e^{low}, T_e^{high}, and T_e^{tail} obtained from the laterally-resolved optical emission spectra after Abel inversion. Despite the localized character of the electron plasma resonance, all values of T_e are radially uniform. This is in sharp contrast to the common local field approximation in which fast electron generation should be limited to the resonance region, i.e. close to the discharge boundaries. In the low-pressure conditions

investigated here, however, since the energy relaxation length of electrons (~2 cm for electrons of average speed 10^8 cm/s and an electron-neutral collision frequency of 2×10^8 s^{-1} in the 50 mTorr, Ar plasma) is larger than the radial size of the reactor (0.6 cm) and of the scale lengths of the spatial inhomogeneity ($\Delta=2\times10^{-4}$ cm), energy transport effects play a crucial role. In such conditions, the local energy absorption by the electrons going through the plasma resonance is redistributed over the whole plasma volume (non-local effect).[33]

To further confirm the precise role of localized plasma resonances on the evolution of the non-local EEDF, TRG-OES measurements were performed for conditions where no surface-wave electric fields are present and thus where no resonance conversion occurs. For surface-wave plasmas sustained in long and narrow dielectric tubes, the electron density decreases along the tube *z*-axis down to the lowest density for which surface-wave propagation is allowed [34]. Beyond this critical point, a field-free region exists where the plasma decays more or less abruptly to zero due to diffusion and convection [28]. In the 50 mTorr, 6 mm i.d. plasma column examined, this field-free region was too short to allow detailed TRG-OES investigations. To circumvent this limitation, a tapered, fused silica discharge tube was used. The plasma was sustain in the small 6 mm diameter segment to ensure that only the azimuthally symmetric surface wave could be excited while plasma emissions were recorded in the large 25 mm diameter region. To maintain the same $n_g\,\Lambda$ scale factor and thus the same mean electron energy as in the previous experiments (see Eq. (1)), the pressure was reduced to 12 mTorr. The axial distribution of the radially-integrated electron number density is presented in Fig. 4 for f=2.45 GHz. TRG-OES measurements were performed both in the microwave-sustained region (within this larger diameter tube) and far in the field-free zone. The corresponding values of T_e^{low}, T_e^{high}, and T_e^{tail} are presented in Table I. In the absence of the surface-wave electric field, the EEDF was

close to a Maxwellian with $T_e^{low} \approx T_e^{high} \approx T_e^{tail} \simeq 4$ eV. On the other hand, in the microwave-sustained region where localized resonant effects occur, the EDDF show again departure from a Maxwellian of temperature $<T_e>$ = 4 eV with a depletion of low-energy electrons given by T_e^{low} and fast electron generation given by T_e^{tail}.

In summary, non-local electron heating of low-energy electrons was observed in low-pressure, argon plasma columns sustained in the microwave regime by electromagnetic surface waves which can be explained by the presence of a plasma resonance near the discharge boundaries. As shown in this Letter, the effect of resonances in the spatially-inhomogeneous plasma appears primarily in the form of a depletion of low-energy electrons due to their acceleration. Electron heating can be ascribed to a wave-particle interaction due to the conversion of surface waves into volume plasmons at the resonance point rather than transit time electron heating across the resonant layer. To the author's knowledge, the present work represents the first experimental evidence of the non-local role of plasma resonances on the EEDF in spatially-inhomogeneous and weakly-collisional microwave discharges.

This research was supported by the National Science and Engineering Research Council (NSERC) and by the National Science Foundation (NSF grant no. CBET-0966967). The authors would like to acknowledge Drs. R. Bravenec, L. Chen, and I. Ghanashev for useful discussions on resonance phenomena.

References

[1] J.Y. Hsu, K. Matsuda, M.S. Chu, and T.H. Jensen, Phys. Rev. Lett. **43**, 203 (1979).

[2] M.M. Turner, Phys. Rev. Lett. **75**, 1312 (1995).

[3] G. Gozadinos, M.M. Turner, and D. Vender, Phys. Rev. Lett. **87**, 135004 (2001).

[4] I. Odrobina, J. Kudela, and M. Kando, Plasma Sources Sci. Technol. **7**, 238 (1998).

[5] M. Moisan, A. Shivarova, and A.W. Trivelpiece, Plasma Phys. **24**, 1331 (1982).

[6] D. Grozev, K. Kirov, K. Makasheva, and A. Shivarova, IEEE Trans. Plasma Sci. **25**, 415 (1997).

[7] A.Y. Lee, Y. Nishida, N.C. Luhmann, Jr., S.P. Obenschain, B. Gu, M. Rhodes, J. R. Albritton, and E. A. Williams, Phys. Rev. Lett. **48**, 319 (1982).

[8] J. Margot and M. Moisan, J. Phys. D:Appl. Phys. **24**, 1765 (1991).

[9] I. Ghanashev, H. Sugai, S. Morita, and N. Toyoda, Plasma Sources Sci. Technol. **8**, 363 (1999).

[10] L.L. Alves, S. Letout, and C. Boisse-Laporte, Phys. Rev. E **79**, 016403 (2009)

[11] Y.M. Aliev, J. Berndt, H. Schlüter, ad A. Shivarova, Plasma Phys. Control. Fusion **36**, 937 (1994)

[12] T. Terebessy, M. Siry, M. Kando, J. Kudela, and D. Korsec, Appl. Phys. Lett. **77**, 2825 (2000).

[13] Y.M. Aliev, V.Y. Bychenkov, A.V. Maximov, and H. Schlüter, Plasma Sources Sci. Technol. **1**, 126 (1992).

[14] I.P. Ganashev and H. Sugai, Plasma Sources Sci. Technol. **11**, A178 (2002).

[15] A. Durandet, Y. Arnal, J. Margot-Chaker, and M. Moisan, J. Phys. D: Appl. Phys. **22**, 1288 (1989).

[16] S. Letout, C. Boisse-Laporte, and L.L. Alves, Appl. Phys. Lett. **89**, 241502 (2006).

[17] J. Kudela, T. Terebessy, and M. Kando, Appl. Phys. Lett. **76**, 1249 (2000).

[18] M. Nagatsu, T. Niwa, and H. Sugai, Appl. Phys. Lett. **81**, 1966 (2002).

[19] S. Nakao, E. Stamate, and H. Sugai, Thin Solid Films **515**, 4869 (2007).

[20] J. Margot-Chaker, M. Moisan, M. Chaker, V.M.M. Glaude, P. Lauque, J. Paraszczak, and G. Sauvé, J. Appl. Phys. **66**, 4134 (1989).

[21] M. Moisan, Z. Zakrzewski, and R. Pantel, J. Phys. D: Appl. Phys. **12**, 219 (1979).

[22] M. Moisan and Z. Zakrzewski, Rev. Sci. Instrum. **58**, 1895 (1987).

[23] V.M. Donnelly, J. Phys. D. Appl. Phys. **37**, R217 (2004).

[24] M.J. Schabel, V.M. Donnelly, A. Kornblit, and W.W. Tai, J. Vac. Sci. Technol. A **20**, 555 (2002).

[25] U. Kortshagen and H. Schlüter, J. Phys. D: Appl. Phys. **25**, 644 (1992).

[26] M.A. Lieberman and A.J. Lichtenberg, *Principles of Plasma Discharges and Materials Processing* (Wiley, New York, 1994).

[27] V. M. Donnelly and M. J. Schabel, J. Appl. Phys. **91**, 6288 (2002).

[28] S. Mattei, O. Boudreault, R. Khare, L. Stafford, and V.M. Donnelly, J. Appl. Phys. **109**, 113304 (2011).

[29] G.J.M. Hagelaar and L.C. Pitchford, Plasma Sources Sci. Technol. **14**, 722 (2005).

[30] V.A. Godyak and V.I. Kolobov, Phys. Rev. Lett. **81**, 369 (1998).

[31] Y.M. Aliev, A.V. Maximov, and H. Schlüter, Phys. Scr. **48**, 464 (1993)

[32] J. Margot and M. Moisan, J. Plasma Phys. **49**, 357 (1993).

[33] I D Kaganovich, V I Demidov, S F Adams, and Y Raitses, Plasma Phys. Control. Fusion **51**, 124003 (2009).

[34] V.M.M. Glaude, M. Moisan, R. Pantel, P. Leprince, and J. Marec, J. Appl. Phys. **51**, 5693 (1981).

Table captions

Table I. Comparison of the electron temperatures determined by TRG-OES in the large portion of the tapered tube for a 2.45 GHz, Ar plasma column.

T_e	Overdense plasma	Expansion region
T_e^{low}	7.9 eV	3.9 eV
T_e^{high}	4.3 eV	4.4 eV
T_e^{tail}	7.9 eV	4.4 eV

Figure captions

Figure 1: Influence of the wave frequency on the values of T_e^{low}, T_e^{high}, and T_e^{tail} determined by TRG-OES in a 50 mTorr, Ar plasma column sustained by surface waves at 4 cm from the end of the plasma column.

Figure 2: Influence of superelastic collisions on the electron energy probability function determined by kinetic simulations.

Figure 3: Radial profiles of T_e^{low}, T_e^{high}, and T_e^{tail} determined by TRG-OES in a 50 mTorr, Ar plasma column sustained by surface waves at 2.45 GHz.

Figure 4: Axial profile of the line-integrated electron number density in a 12 mTorr, Ar plasma column sustained by surface waves at 2.45 GHz. Measurements were performed in the larger portion of a tapered fused silica discharge tube. Electron densities were obtained from phase-sensitive microwave interferometry in the microwave-sustained region and optical emission spectroscopy in the field-free zone (see ref. 28 for details).

Figure 1

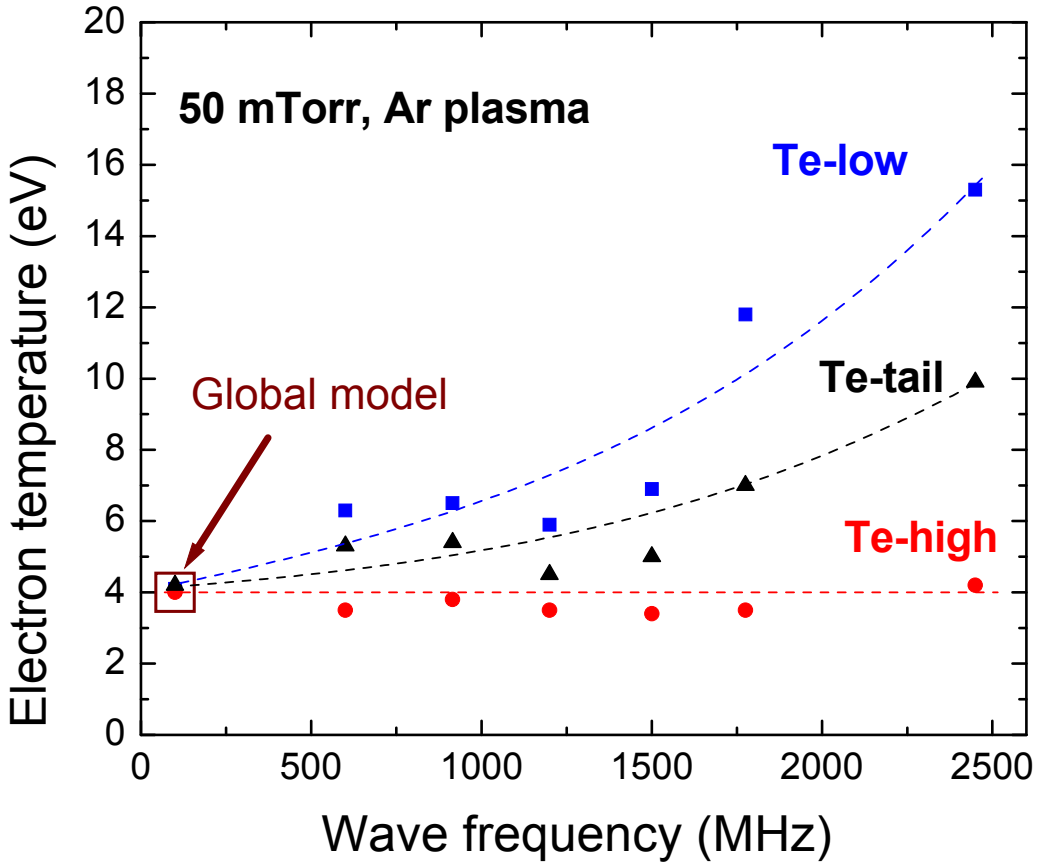

Boudreault et al.

Figure 2

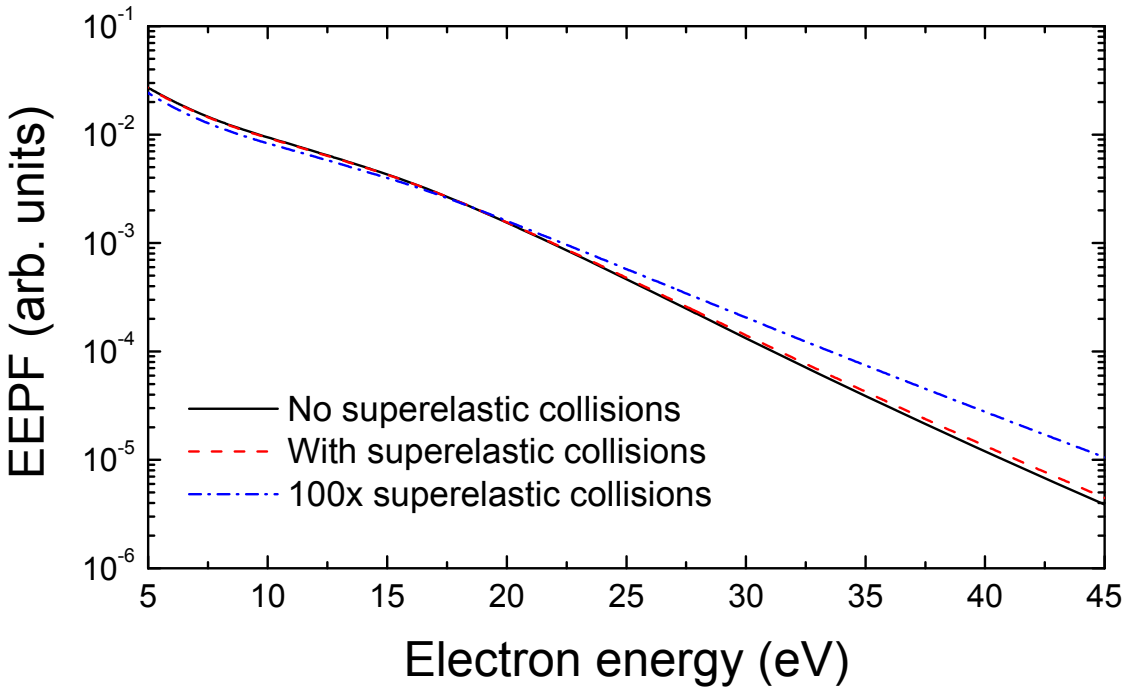

Boudreault et al.

Figure 3

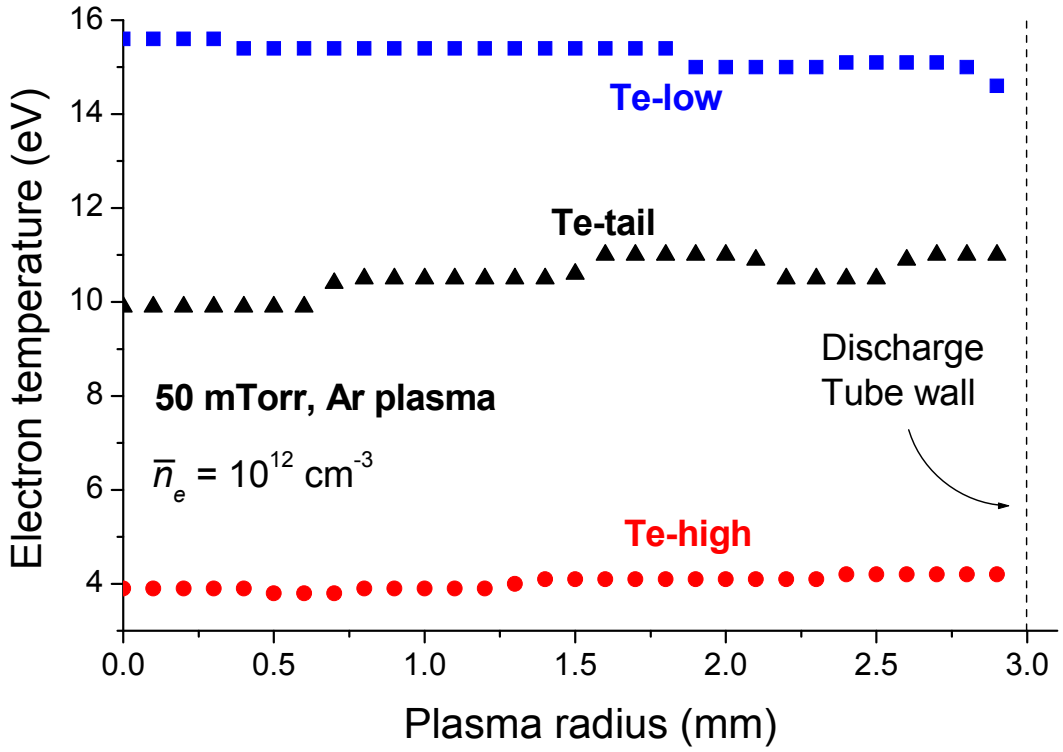

Boudreault et al.

Figure 4

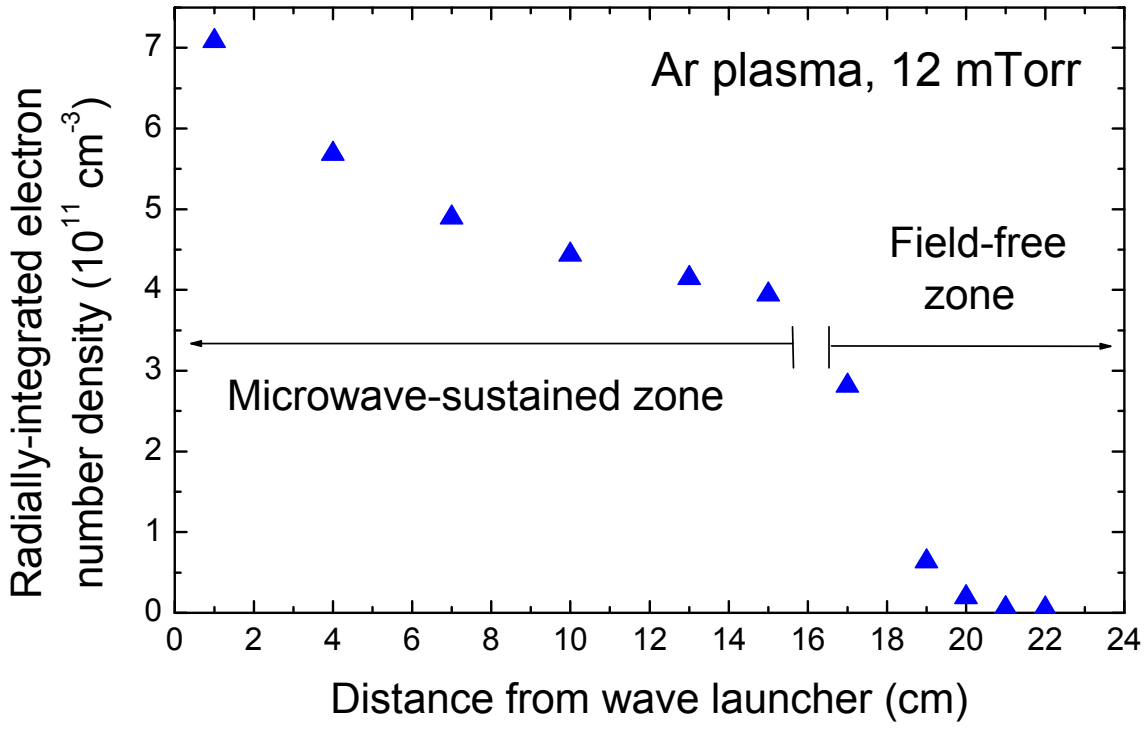

Boudreault et al.